Downloaded from orbit.dtu.dk on: Apr 26, 2024

DTU Library

Influence of pump beam shaping and noise on performance of a direct diode-pumped ultrafast Ti:sapphire laser

Jamal, Muhammad Tahir; Hansen, Anders Kragh; Tawfieq, Mahmoud; Andersen, Peter Eskil; Jensen, Ole Bjarlin

Published in:
Optics Express

Link to article, DOI:
10.1364/OE.404968

Publication date:
2020

Document Version
Publisher's PDF, also known as Version of record

Link back to DTU Orbit

Citation (APA):
Jamal, M. T., Hansen, A. K., Tawfieq, M., Andersen, P. E., & Jensen, O. B. (2020). Influence of pump beam shaping and noise on performance of a direct diode-pumped ultrafast Ti:sapphire laser. *Optics Express*, *28*(21), 31754-31762. https://doi.org/10.1364/OE.404968

General rights
Copyright and moral rights for the publications made accessible in the public portal are retained by the authors and/or other copyright owners and it is a condition of accessing publications that users recognise and abide by the legal requirements associated with these rights.

- Users may download and print one copy of any publication from the public portal for the purpose of private study or research.
- You may not further distribute the material or use it for any profit-making activity or commercial gain
- You may freely distribute the URL identifying the publication in the public portal

If you believe that this document breaches copyright please contact us providing details, and we will remove access to the work immediately and investigate your claim.

Research Article | Vol. 28, No. 21 / 12 October 2020 / Optics Express 31754

Optics EXPRESS

Influence of pump beam shaping and noise on performance of a direct diode-pumped ultrafast Ti:sapphire laser

MUHAMMAD TAHIR JAMAL,[1,*] ANDERS KRAGH HANSEN,[2] MAHMOUD TAWFIEQ,[1] PETER ESKIL ANDERSEN,[1] AND OLE BJARLIN JENSEN[2]

[1] DTU Health Tech, Technical University of Denmark, Frederiksborgvej 399, 4000 Roskilde, Denmark
[2] DTU Fotonik, Technical University of Denmark, Frederiksborgvej 399, 4000 Roskilde, Denmark
[*] mutaj@dtu.dk

Abstract: One of the major factors that limits the widespread use of ultrafast titanium sapphire (Ti:S) lasers in life science is its expensive and complex pump source. Broad area diode laser (BA-DL) based pump sources have high potential to solve this problem, since they are compact, inexpensive and very efficient. However, their non-diffraction limited beam profile makes it challenging to achieve high powers in Kerr-lens mode-locked (KLM) operation of Ti:S lasers. In this work, we show that the ideal way to beam shape two spectrally combined BA-DLs with different beam qualities is to aim for a compromise between matching to the cavity mode diameter and the cavity mode Rayleigh range. We furthermore conclude that the relative intensity noise (RIN) of the BA-DL pumped Ti:S laser, another important parameter for imaging applications, is sufficiently low for a wide range of life science applications. However, for applications that are highly sensitive to noise, new laser diode designs are likely necessary to reduce inherent noise originating within the laser diode.

© 2020 Optical Society of America under the terms of the OSA Open Access Publishing Agreement

1. Introduction

Having the capability of generating femtosecond pulses with broad spectral tuning range starting from ~650-1100 nm, the ultrafast Ti:S lasers play a major role in the development of many biophotonic imaging technologies, like optical coherence tomography [1–3] and multiphoton imaging [4–6], for the diagnosis of different types of early stage cancers [7–9]. In these applications, the intensity noise of the Ti:S laser play an important role in order to achieve a high signal-to-noise level and good image contrast [10,11] Traditionally, frequency-doubled diode-pumped solid-state lasers (DPSSLs) operating in the green wavelength region have been used for pumping of the Ti:S lasers. These commercial DPSSLs are preferred due to their high output power with excellent beam quality and low relative intensity noise (RIN); however, they are expensive, complex with large footprint and have very low wall-plug efficiency, i.e. ~2.5%. These are the major factors that limits the widespread use of Ti:S lasers for biophotonic imaging in life science and health care applications. High power blue-green diode lasers are comparatively much more efficient (wall-plug efficiency ~15-50%), compact and can be produced in high volume at comparatively very low cost [12]. Recent progress in broad area diode laser (BA-DL) technology [13,14] in the wavelength region suitable for Ti:S pumping has provided the opportunity of the development of inexpensive BA-DL based pump sources. The first BA-DL pumped Ti:S CW operation was demonstrated in 2009 by Roth *et al.* [15]. Since then several embodiments of BA-DL pumped Ti:S in Kerr-lens mode-locked (KLM) operation have been reported [16–20]. In Ref. [18], the influence of BA-DL pump beam shaping only along the fast axis was reported. Gürel *et al.* [21]. and Castro-Marin *et al.* [22]. have demonstrated the carrier-envelope-offset frequency (f_{CEO}) stabilization of a BA-DL pumped SESAM mode-locked

#404968 https://doi.org/10.1364/OE.404968
Journal © 2020 Received 11 Aug 2020; revised 25 Sep 2020; accepted 28 Sep 2020; published 6 Oct 2020

Optics EXPRESS

Ti:S laser by modulation of a green (520 nm) BA-DL and a blue (462 nm) BA-DL, respectively. They have discussed the influence of the BA-DL intensity noise mainly on the phase noise of the f_{CEO} stabilized SESAM mode-locked Ti:S laser. The first green (520 nm) BA-DL pumped Ti:S was reported in [23] and further power scaling using similar green BA-DLs was reported in Ref. [19], where the authors overdrove the green BA-DLs to achieve higher power. However, overdriving of these BA-DLs reduces their lifetime. Although the blue (450-472 nm) BA-DLs can give up to 5 W per emitter, pump-induced losses have often been observed when these BA-DLs were used for pumping [15,24]. Sugiyama *et al.* [20]. have reported power scaling using wavelength multiplexing of 520 nm and 478 nm BA-DLs without any pump induced losses. The recently developed watt-level cyan BA-DL with $\lambda_c = 488$ nm is closest to the peak of the absorption curve of Ti:S crystal, i.e. 490 nm, among the rest of the watt-level BA-DLs which makes it a very attractive candidate for pumping.

In this paper, we have investigated the optimum pump beam shaping of wavelength beam combined cyan and green BA-DLs with significantly different beam properties. We achieve a slope efficiency close to that achievable using a solid-state laser. Furthermore, we study the influence of the intensity noise of the BA-DL on the intensity noise of the Ti:S laser and find a relatively low intensity noise despite high intensity noise in the BA-DL based pump laser. The intensity noise of BA-DL pumped Ti:S is not far from the frequency-doubled tapered laser pumped Ti:S, which makes the BA-DL pumped Ti:S laser a good candidate for bio-imaging [25].

2. Compact laser setup

The schematic diagram of the experimental setup is shown in Fig. 1. Both BA-DLs (Nichia) were operated at room temperature and no temperature stabilization scheme was implemented. 2 W of output power from a cyan BA-DL was spectrally combined with 0.9 W output power from a green BA-DL using a dichroic mirror. Different emitter widths of the green and the cyan BA-DL,

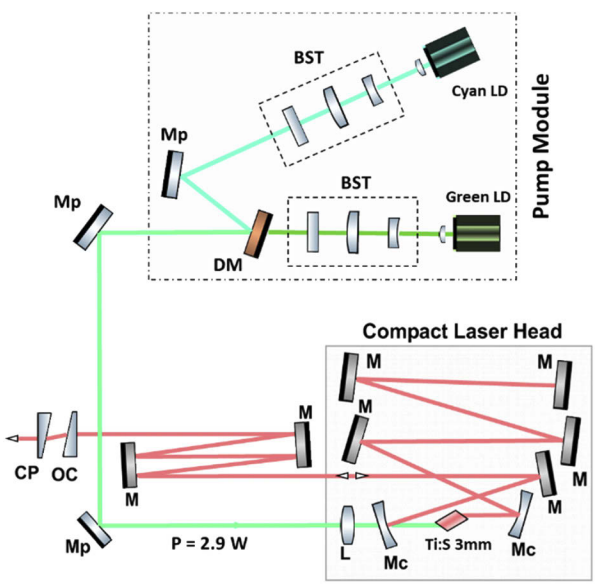

Fig. 1. Schematic diagram of a compact Ti:sapphire laser pumped with a spectrally combined cyan and green BA-DL pump module. LD: laser diode; CL: collimation lens; BST: beam shaping telescope; DM: dichroic mirror; Mp: pump mirror; L: coupling lens; Mc: folding mirror; M: dispersion compensation mirror; OC: output coupler; CP: compensation plate.

Optics EXPRESS

i.e. 15 µm and 25 µm, respectively, cause them to have different maximum output power and beam properties.

A Galilean telescope with three lenses was implemented as a beam shaper along both the slow and the fast axes (SA and FA, respectively) and several combinations of lenses were used in order to realize different beam shapes for pumping. After the dichroic mirror, the combined beam was focused by a 40 mm focal length lens into a 3 mm long Ti:S crystal mounted in an astigmatism-compensated, asymmetrically x-folded cavity with f = -25 mm folding–focusing mirrors. The focus diameter of the cavity mode in the Ti:S crystal was approximately 33.5 µm along the SA and 20 µm along FA, accounting for the Brewster angle crystal. Here the SA is parallel to the optical table. To compensate for second and third-order dispersion of the laser crystal and air, low-loss resonant dispersive chirped mirrors were used. One mirror pair was used in a double-pass configuration in order to minimize the overall size. The KLM operation was initiated by intensity fluctuations from translational perturbation of the end mirror.

3. BA-DLs pump beam shaping

The non-diffraction-limited and different beam quality of the BA-DLs along the SA makes it challenging to achieve optimum mode matching. The beam propagation factor M^2 (4σ) of the green and the cyan BA-DL along SA was measured to be 4.5 and 8.7, respectively, and ~1.5 along FA for both BA-DLs. The SA divergence of the green BA-DL is 8.2° and for the cyan it is 13°. The optimum mode matching which is basically a delicate balance between the focused spot size matching and the divergence matching inside the Ti:S crystal, can still be obtained with such multimode BA-DLs by careful beam shaping. Since these BA-DLs have comparatively better beam quality along the FA than the SA, it is relatively easier to mode match along the FA. Therefore, we keep the FA diameter of the BA-DLs constant at the experimentally determined optimum level. Thereby, we can study the effect of the SA beam diameter on the pumping efficiency of the Ti:S laser. The optimization of each BA-DL beam was performed independently, while the other pump source was turned off.

3.1. Results and discussion

The maximum CW output power of the Ti:S laser for each individual BA-DL as a function of the SA focused beam diameter inside the Ti:S crystal is shown in Fig. 2. The beam diameter values of both BA-DLs and the Ti:S laser inside the Ti:S crystal were obtained from simulations done in the ray tracing software BeamXpertDESIGNER [26] using measured parameters of the setup shown in Fig. 1. For both BA-DLs, an elliptical beam with the SA focal diameter (D_G = 43 µm, D_C = 55 µm) almost twice as large as the FA focal diameter, gives the maximum output power of the Ti:S laser, indicating the optimum coupling between the pump and the resonator mode. The difference between the optimum focal diameters of these BA-DLs is due to the difference in their beam quality. The optimum focal diameters for both BA-DLs were found to be at the point where their matching Rayleigh lengths ~1.2 mm were very close to the Rayleigh length of the cavity mode ~1.5 mm. Overlap integral calculations between the cavity mode and the pump modes shown in Fig. 2(b) show optimum SA focal diameters of D_G = 42 µm, D_C = 53 µm in good agreement with the experiments.

The Ti:S output power decreases by further increasing the SA focal diameter from the optimum value because the pump power density reduces too much thereby decreasing the pumping efficiency. By further decreasing the SA beam diameter to match the mode focal diameter, the higher divergence of the pump worsens the overlap with the cavity mode and results in lower pump efficiency, see Fig. 2(b). This is in contrast to high gain solid state laser materials, where a larger pump beam will give rise to higher order transverse modes [27]. We did not observe any higher order modes in our Ti:S laser, which we believe is explained by the significantly higher threshold power density of the Ti:S material that is determined by its short carrier lifetime. The

Optics EXPRESS

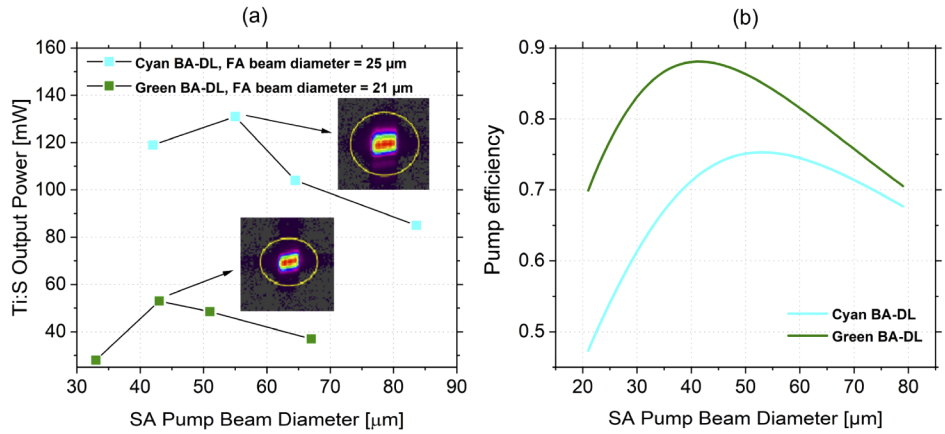

Fig. 2. a) The maximum CW output power of the Ti:S laser as a function of SA focused beam diameters of the cyan and green BA-DLs. Both BA-DLs were operated at their maximum power i.e. PG = 0.9 W and PC = 2 W. The insets show the focused beam profiles from a beam profiler. b) Pump efficiency, obtained from overlap integral, showing good agreement with data in (a).

absorption properties of Ti:S crystal used in this are given in Table 1. The absorbed power is 4.2% higher at 515 nm and 8.7% higher at 488 nm compared to 532 nm.

Table 1. Measured absorption properties of Ti:S crystal at three wavelengths.

Wavelengths	488 nm	515 nm	532 nm
Absorption [%]	82.1	77.6	73.4
Absorption coefficient [cm^{-1}]	5.73	2.2	2

We demonstrated a maximum CW output power of 270 mW and stable KLM output power of 190 mW from a combined pump power of $P_C + P_G = 2.9$ W. The efficiency and performance of the BA-DL pumped Ti:S was compared to a DPSSL (Verdi V5, *Coherent*) pumped Ti:S, shown in Figs. 3(a) and 3(b), under CW and KLM operation, respectively. The DPSSL is capable of emitting a diffraction-limited beam at 532 nm. In case of DPSSL pumping, the optical-optical (OO) conversion efficiency was 13% and 7.8% for CW and KLM operations, respectively. In case of our BA-DL pump, we were able to achieve an OO conversion efficiency of 9.2% and 6.5% in CW and KLM operations, respectively. Taking the higher wall-plug efficiency of BA-DLs into account, the overall efficiency of diode laser pumping is significantly higher than DPSSL laser pumping [28], see Table 2.

Table 2. Comparison of OO, slope and wall-plug efficiency of the two pumping schemes under CW and KLM operation.

Ti:S pump type	DPSSL (Verdi)		BA-DL	
Lasing operation	CW	KLM	CW	KLM
OO conversion efficiency [%]	13.0	7.8	9.2	6.5
Slope efficiency [%]	15.5	9.8	13.0	9.7
Wall-plug efficiency [%]	0.06	0.04	1.6	1.2

The OO conversion efficiency, the slope efficiency (SE) and the wall-plug efficiency comparison for both pumping schemes is shown in Table 2. The SE under KLM operation is almost the same

Optics EXPRESS

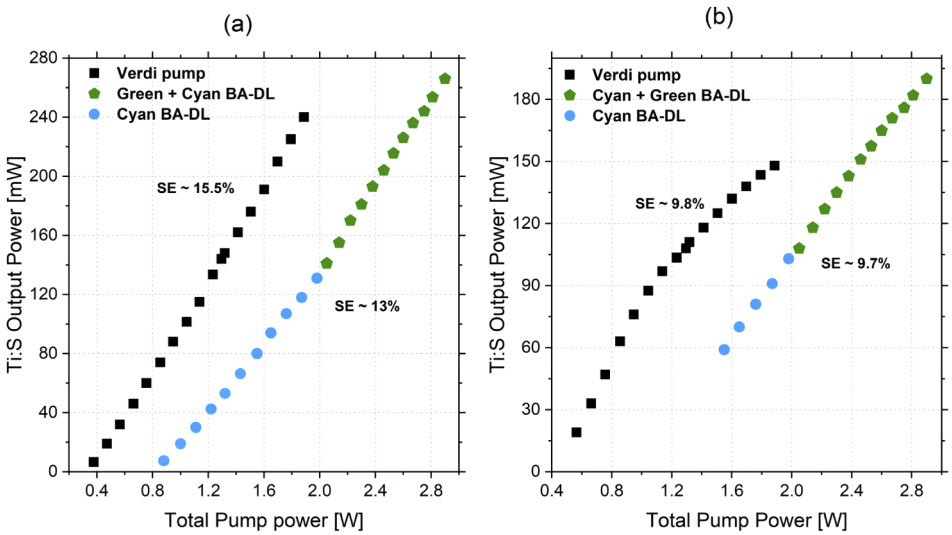

Fig. 3. Comparison of Ti:S output power in (a) CW operation and (b) KLM operation when pumped with a commercial DPSSL pump (black squares) and spectrally combined cyan and green (cyan dots and green pentagons) BA-DLs pump module.

for both cases of Ti:S pumping. However, there is a noticeable difference in lasing threshold under both CW and KLM operation despite the fact that the cyan (488 nm) and the green (517 nm) BA-DLs' wavelengths have higher absorption efficiency than the green (532 nm) DPSSL's wavelength. This can be explained by the adverse effects of poor beam quality that dominate the advantage of slightly higher absorption efficiency of the BA-DLs' wavelengths compared to DPSSL wavelength.

With a centre wavelength of 806 nm, we measured a spectral width of $\Delta\lambda_{\mathrm{FWHM}} = 35.5$ nm and a pulse duration of 30 fs using FROG (GRENOUILLE, *Swamp Optics*).

4. Noise characterization

4.1. Setup for optical noise measurement

We used the homodyne detection system shown in Fig. 4 to characterize the optical intensity noise. This setup is similar to the one described in Ref. [29]. The power of the input laser beam was adjusted using a continuously variable neutral density (ND) filter, while the combination of a half-wave plate and a polarizing beam splitter (PBS) was used to control the power impinging on each photodiode of the balanced amplified photodetector (BAP) module (PDB450-AC, *Thorlabs*).

The BAP module has two Si-based well-matched photodiodes attached to an ultra-low noise, high-speed transimpedance amplifier that generates an output voltage (RF output). The RF output voltage is proportional to the difference between the photocurrents, generated by the incident laser beam in the two photodiodes. The broad detection bandwidth of the Si-based photodiodes (320-1000 nm) covers the emission spectra of both BA-DLs and Ti:S laser. Hence, using the same BAP module for the noise measurement of the BA-DL pump module as well as the Ti:S output offers a convenient and reliable way for comparison. The optical elements like half waveplate and PBS were replaced according to the wavelength compatibility. The BAP module has two monitor outputs to measure the incident optical power level at each photodiode individually. We measured the two monitor voltages with an oscilloscope while the RF output was connected to a virtual spectrum analyzer (VSA) in order to measure the power spectral density (PSD). The VSA was realized by using a PicoScope 2206B oscilloscope combined with the signal processing

Optics EXPRESS

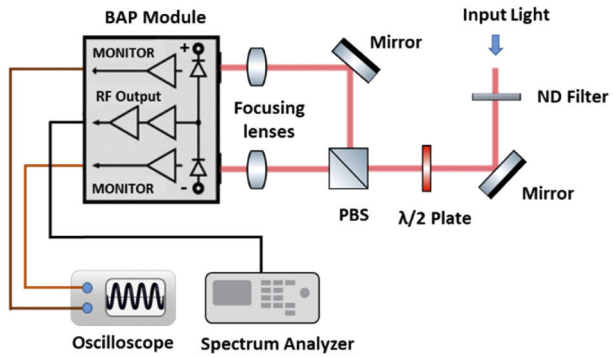

Fig. 4. Setup used for the measurement of optical intensity noise.

of its time trace signal to obtain the PSD. The bandwidth of the PicoScope is 50 MHz and the bandwidth of the transimpedance amplifier is 45 MHz at the chosen gain setting of $A_g = 0.5 \times 10^4$ V/A, enough to cover the region of interest.

The RF output gives the amplitude noise when the laser beam impinges only on one of the photodiodes of the BAP module. When the input beam is split into two and equal power impinges on each photodiode of the BAP module, the RF output provides the experimental shot noise. The good agreement of the experimental shot noise level with the theoretical shot noise level validates the reliability of the noise measurement setup. The theoretical shot noise limit was calculated using standard equations reported in [10].

In order to characterize the performance of the noise measurement setup, noise levels contributed by the background sources, i.e. VSA and BAP module, were obtained and are shown in Fig. 5 along with the experimental shot noise and amplitude noise of a BA-DL. Furthermore, Fig. 5 shows that below 3 kHz, the background noise coming from the measurement setup exceeds the shot noise. The prominent noise features appearing around 300 kHz in magenta curve are intrinsic to the BAP module. However, we ensured that the overall background noise level of the noise measurement setup is low enough to not limit the shot noise measurement of each laser. The measured common mode rejection ratio is larger than 25 dB.

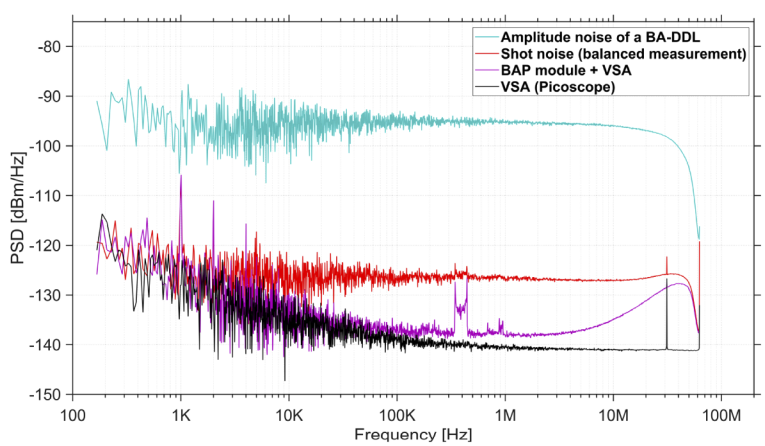

Fig. 5. PSD plot showing the noise levels of background sources, i.e. VSA (black), VSA plus the BAP module (Magenta), and experimental shot noise (red) and amplitude noise of the cyan BA-DDL. The bandwidth of the BAP module is 45 MHz.

Optics EXPRESS

4.2. Results and discussion

The amplitude noise of both the cyan and the green BA-DLs and the KLM Ti:S laser, measured as PSD, is shown in Fig. 6. In order to compare the amplitude noise of lasers having different wavelengths and optical powers, the unit of the y-axis was converted from dBm/Hz to dBc/Hz by normalizing the PSD relative to the carrier, the mean power. The respective RIN rms values were obtained by integrating the normalized PSD over an interval of [100-1M] Hz and are given in Table 3. Both BA-DLs showed strong white noise with flat noise floor of −120 dBc/Hz extending up to 40 MHz. To explain this behavior we looked into various potential sources of noise. Several power supplies with different electrical noise features were used to drive each BA-DL in order to identify if this high white noise is caused by the electrical noise originating from the power supply. All the tested power supplies showed moderate electrical noise in the [100-100k] Hz region but showed very low noise reaching to the background noise level above 300 kHz. Hence, the high white noise of BA-DLs above 300 kHz cannot be attributed to the electrical noise of power supplies. There are several other possibilities for the origin of this high white noise level. We hypothesize that the high white noise level of the BA-DLs is caused by longitudinal or transverse mode competition. Longitudinal mode competition has been shown to cause excess and flat intensity noise at low frequencies in single-mode diode lasers [30,31]. In a BA-DL operated far above threshold several spatial modes oscillate and competition between these modes may give rise to the observed increased intensity noise.

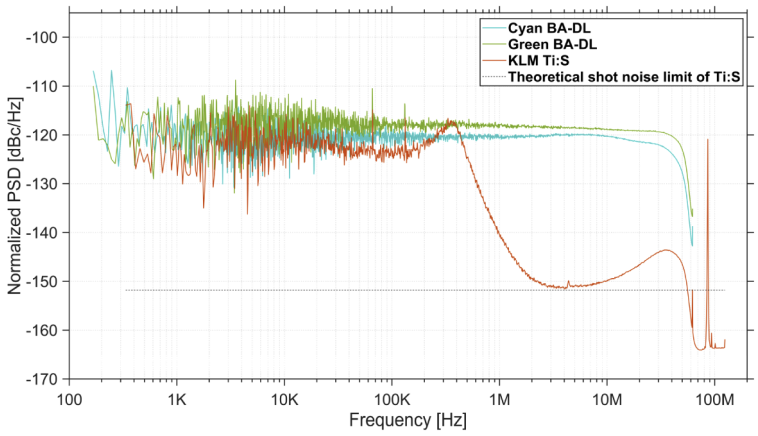

Fig. 6. Normalized PSD plot showing the amplitude noise of both, cyan and green, BA-DDLs and the mode-locked Ti:S laser.

Table 3. Comparison of the RIN rms values of three different pump lasers and the KLM Ti:S laser pumped by these lasers.

Type	Pump source RIN rms %	KLM Ti:S RIN rms %
DPSSL (Verdi V5) [10]	0.0056	0.0076
Frequency-doubled tapered laser [10]	0.038	0.047
Cyan LD, Green LD	0.096, 0.125	0.070

The Ti:S shows a broad peak around 400 kHz, presumably originating from relaxation oscillation frequencies (ROF), matching well with the expectations for a pump power of 2.9 W according to the literature [29]. The ROF peak is followed by the cutoff frequency corresponding to the upper state lifetime (3.2 µs) of the Ti:S. The noise spectrum of Ti:S in the region above 2 MHz, was observed to be limited by the shot noise level, i.e. −152 dBc/Hz. The broader noise

Optics EXPRESS

peak appearing around 40 MHz is originating from the amplifier of the BAP module, a feature still observed when the laser is off. Since the cutoff frequency of the BAP module is 45 MHz, beyond this frequency the noise amplitude starts to drop and does not represent the actual noise level anymore. The sharp peak appearing at 86 MHz is the repetition rate of the Ti:S laser.

The lower noise of the Ti:S laser in the region below its cutoff frequency, compared to BA-DLs noise points towards two theories that can potentially explain such behavior: 1) The noise originating from longitudinal mode competition is being suppressed due to the broad gain bandwidth of the Ti:S crystal. 2) The noise of the higher order spatial modes has much less contribution in the Ti:S output noise compared to the fundamental mode noise due to their lower spatial overlap with the cavity mode. However, due to technical limitations these theories were not verified in this work.

Table 3 shows the comparison of the RIN rms values (integrated over [100-1M] Hz) of three different pump lasers and the same KLM Ti:S laser when pumped with these three pump lasers.

The DPSSL has the lowest noise which unsurprisingly results in the lowest Ti:S noise. Although the BA-DLs exhibits the highest noise, the noise performance they provide from KLM Ti:S laser is not far from the noise performance of the frequency-doubled tapered laser pumped Ti:S laser. For applications that require an extremely low noise Ti:S laser, the high inherent noise of the BA-DLs is an obstacle that needs to be addressed, probably on a device design and fabrication level, before BA-DL can be used as a suitable pump source.

5. Conclusion

In this work, it has been shown that careful beam shaping before wavelength-multiplexing of two BA-DLs with very different beam qualities leads to efficient pumping of a KLM Ti:S laser. The highest output power of the Ti:S laser was achieved when the Rayleigh range of both BA-DLs were matched and were slightly less than the Rayleigh length of the cavity mode inside the Ti:S crystal. The best pumping efficiency is achieved at a compromise between matching to the cavity mode diameter and the cavity mode Rayleigh range.

The Ti:S laser has shown some degree of robustness to the noise of the BA-DL based pump by showing less RIN compared to the BA-DL pump RIN. The comparison of Ti:S performance with different pumps shows that BA-DL pumped Ti:S RIN is higher than RIN of the DPSSL pumped Ti:S, however it is comparable to the RIN of frequency-doubled tapered laser pumped Ti:S laser that has already shown good performance for multiphoton imaging. These results imply that BA-DLs, which offer less expensive, compact and much simpler pumping schemes, as an alternative to some of the commercially available DPSSLs, can enable simple and affordable Ti:S systems and make them more available for biomedical applications.

Funding

H2020 Marie Skłodowska-Curie Actions (721766).

Disclosures

The authors declare no conflicts of interest.

References

1. T. Schmoll, A. Unterhuber, C. Kolbitsch, T. Le, A. Stingl, and R. Leitgeb, "Precise Thickness Measurements of Bowman's Layer, Epithelium, and Tear Film," Optom. Vis. Sci. **89**(5), E795–E802 (2012).
2. R. M. Werkmeister, A. Alex, S. Kaya, A. Unterhuber, B. Hofer, J. Riedl, M. Bronhagl, M. Vietauer, D. Schmidl, T. Schmoll, G. Garhöfer, W. Drexler, R. A. Leitgeb, M. Groeschl, and L. Schmetterer, "Measurement of Tear Film Thickness Using Ultrahigh-Resolution Optical Coherence Tomography," Invest. Ophthalmol. Visual Sci. **54**(8), 5578–5583 (2013).

Optics EXPRESS

3. A. Unterhuber, B. Považay, B. Hermann, H. Sattmann, W. Drexler, V. Yakovlev, G. Tempea, C. Schubert, E. M. Anger, P. K. Ahnelt, M. Stur, J. E. Morgan, A. Cowey, G. Jung, T. Le, and A. Stingl, "Compact, low-cost Ti:Al2O3 laser for in vivo ultrahigh-resolution optical coherence tomography," Opt. Lett. **28**(11), 905–907 (2003).
4. A. Rohrbacher, O. E. Olarte, V. Villamaina, P. Loza-Alvarez, and B. Resan, "Multiphoton imaging with blue-diode-pumped SESAM-modelocked Ti:sapphire oscillator generating 5 nJ 82 fs pulses," Opt. Express **25**(9), 10677 (2017).
5. M. E. Dickinson, E. Simbuerger, B. Zimmermann, C. W. Waters, and S. E. Fraser, "Multiphoton excitation spectra in biological samples," J. Biomed. Opt. **8**(3), 329–339 (2003).
6. F. Helmchen and W. Denk, "Deep tissue two-photon microscopy," Nat. Methods **2**(12), 932–940 (2005).
7. I. Pavlova, K. R. Hume, S. A. Yazinski, J. Flanders, T. L. Southard, R. S. Weiss, and W. W. Webb, "Multiphoton microscopy and microspectroscopy for diagnostics of inflammatory and neoplastic lung," J. Biomed. Opt. **17**(3), 036014 (2012).
8. L. Perrin, B. Bayarmagnai, and B. Gligorijevic, "Frontiers in intravital multiphoton microscopy of cancer," Cancer Rep. (N. Y., NY, U. S.) **3**, e1192 (2020).
9. L. Li, D. Kang, Z. Huang, Z. Zhan, C. Feng, Y. Zhou, H. Tu, S. Zhuo, and J. Chen, "Multimodal multiphoton imaging for label-free monitoring of early gastric cancer," BMC Cancer **19**(1), 295 (2019).
10. M. Tawfieq, "Noise Transfer from Laser Sources to Bio-images," Master Thesis, DTU Fotonik, Technical University of Denmark (2015).
11. D. Marti, M. Djurhuus, O. B. Jensen, and P. E. Andersen, "Multi-photon microscope driven by novel green laser pump," Proc. SPIE **9712**, 97121M (2016).
12. Laser diode source, "How much do laser diodes cost?," https://www.laserdiodesource.com/how-much-does-a-laser-diode-cost.
13. S. Masui, T. Miyoshi, T. Yanamoto, and S. Nagahama, "1 W AlInGaN based green laser diodes," in *Conference on Lasers and Electro-Optics Pacific Rim (CLEOPR)* (IEEE, 2013), pp. WH3-1.
14. L. Jiang, J. Liu, A. Tian, Y. Cheng, Z. Li, L. Zhang, S. Zhang, D. Li, M. Ikeda, and H. Yang, "GaN-based green laser diodes," J. Semicond. **37**(11), 111001 (2016).
15. P. W. Roth, A. J. Maclean, D. Burns, and A. J. Kemp, "Directly diode-laser-pumped Ti:sapphire laser," Opt. Lett. **34**(21), 3334–3336 (2009).
16. C. G. Durfee, T. Storz, J. Garlick, S. Hill, J. A. Squier, M. Kirchner, G. Taft, K. Shea, H. Kapteyn, M. Murnane, and S. Backus, "Direct diode-pumped Kerr-lens mode-locked Ti:sapphire laser," Opt. Express **20**(13), 13677 (2012).
17. S. Backus, M. Kirchner, C. Durfee, M. Murnane, and H. Kapteyn, "Direct diode-pumped Kerr Lens 13 fs Ti:sapphire ultrafast oscillator using a single blue laser diode," Opt. Express **25**(11), 12469 (2017).
18. D. A. Kopylov, M. N. Esaulkov, I. I. Kuritsyn, A. O. Mavritskiy, B. E. Perminov, A. V. Konyashchenko, T. V. Murzina, and A. I. Maydykovskiy, "Kerr-lens mode-locked Ti:Sapphire laser pumped by a single laser diode," Laser Phys. Lett. **15**(4), 045001 (2018).
19. K. Gürel, V. J. Wittwer, M. Hoffmann, C. J. Saraceno, S. Hakobyan, B. Resan, A. Rohrbacher, K. Weingarten, S. Schilt, and T. Südmeyer, "Green-diode-pumped femtosecond Ti:Sapphire laser with up to 450 mW average power," Opt. Express **23**(23), 30043 (2015).
20. N. Sugiyama, H. Tanaka, and F. Kannari, "Mode-locked Ti:sapphire laser oscillators pumped by wavelength-multiplexed laser diodes," Jpn. J. Appl. Phys. **57**(5), 052701 (2018).
21. K. Gürel, V. J. Wittwer, S. Hakobyan, S. Schilt, and T. Südmeyer, "Carrier envelope offset frequency detection and stabilization of a diode-pumped mode-locked Ti:sapphire laser," Opt. Lett. **42**(6), 1035 (2017).
22. P. Castro-Marin, T. Mitchell, J. Sun, and D. T. Reid, "Characterization of a carrier-envelope-offset-stabilized blue- and green-diode-pumped Ti:sapphire frequency comb," Opt. Lett. **44**(21), 5270–5273 (2019).
23. S. Sawai, A. Hosaka, H. Kawauchi, K. Hirosawa, and F. Kannari, "Demonstration of a Ti: sapphire mode-lock laser pumped directly with a green diode laser," Appl. Phys. Express **7**(2), 022702 (2014).
24. R. Sawada, H. Tanaka, N. Sugiyama, and F. Kannari, "Wavelength-multiplexed pumping with 478- and 520-nm indium gallium nitride laser diodes for Ti:sapphire laser," Appl. Opt. **56**(6), 1654–1661 (2017).
25. D. Marti, M. Djurhuus, O. B. Jensen, and P. E. Andersen, "Multi-photon microscope driven by novel green laser pump," in *Multiphoton Microscopy in the Biomedical Sciences XVI*, A. Periasamy, P. T. C. So, and K. König, eds. (SPIE, 2016), 9712, pp. 174–178.
26. BeamXpert, "Simulation of Laser Radiation - BeamXpertDESIGNER," https://www.beamxpert.com/en.
27. W. Koechner, *Solid-State Laser Engineering*, 6th ed., Springer Series in Optical Sciences (Springer-Verlag, 2006).
28. Laser Focus World, "Photonic Frontiers: High-efficiency Optical Pumping: "Going green" cranks up the laser power," https://www.laserfocusworld.com/lasers-sources/article/16547048/photonic-frontiers-highefficiency-optical-pumping-going-green-cranks-up-the-laser-power.
29. M. Tawfieq, A. K. Hansen, O. B. Jensen, D. Marti, B. Sumpf, and P. E. Andersen, "Intensity Noise Transfer Through a Diode-pumped Titanium Sapphire Laser System," IEEE J. Quantum Electron. **54**(1), 1–9 (2018).
30. M. Yamada, "Theory of mode competition noise in semiconductor injection lasers," IEEE J. Quantum Electron. **22**(7), 1052–1059 (1986).
31. S. M. S. Imran, M. Yamada, and Y. Kuwamura, "Theoretical Analysis of the Optical Feedback Noise Based on Multimode Model of Semiconductor Lasers," IEEE J. Quantum Electron. **48**(4), 521–527 (2012).